Synthesis and Self-Assembly of Amphiphilic Dendrimers Based on Aliphatic Polyether-Type Dendritic Cores

Byoung-Ki Cho, Anurag Jain, Jörg Nieberle,† Surbhi Mahajan, and Ulrich Wiesner*

Department of Materials Science and Engineering, Cornell University, Ithaca, New York 14853

Sol M. Gruner

Department of Physics, Cornell University, Ithaca, New York 14853

Stephan Türk and Hans Joachim Räder

Max Planck Institute for Polymer Research, Ackermannweg 10, 55128 Mainz, Germany

Received November 20, 2003; Revised Manuscript Received February 22, 2004

ABSTRACT: We have prepared a series of amphiphilic dendrimers with hydrophilic aliphatic polyether-type dendritic core and hydrophobic docosyl peripheries. All dendrimers from first up to fourth generation **1**−**4** were synthesized in good yield and high purity by a stepwise convergent approach consisting of a combination of Williamson etherification and hydroboration/oxidation steps. Differential scanning calorimetry (DSC) measurements show that the docosyl peripheries melting temperatures and corresponding heats of fusion decrease only slightly with each generation, indicative of a strong segregation between hydrophilic dendritic core and hydrophobic docosyl periphery. The DSC derived docosyl periphery crystallinity shows a gradual reduction with each generation and is corroborated by wide-angle X-ray scattering (WAXS) experiments. Amphiphilic dendrimer self-assembly in the solid state is investigated by small-angle X-ray scattering. Data from **1**, **2**, and **3** suggest a bilayer lamellar structure with interdigitated dendritic core packing. In contrast, data from **4** are consistent with a 2-dimensional oblique columnar assembly with hydrophilic core structure. The observed thermal and morphological behaviors are rationalized in terms of high incompatibility and intrinsic interfacial curvature between hydrophilic dendritic core and hydrophobic docosyl periphery arising from the unique dendritic molecular architecture.

Introduction

Molecular amphiphiles have great application potential, e.g., as nanocarriers,[1] as structure directing agents for nanostructure formation,[2] or in catalysts.[3] Recently, macromolecular amphiphiles made from linear-type block copolymers with various molecular compositions have been extensively studied due to their simple architecture and facile synthetic accessibility.[2b−f,4] In these systems poly(ethylene oxide) (PEO) has been widely used as the hydrophilic component because of its high polarity, ion-transporting ability, and biocompatibility, resulting in self-assembling materials,[4] ion-conducting polyelectrolytes,[5] and drug-delivery[6] applications. Typical examples for the hydrophobic block incompatible with PEO are polystyrene,[4a,b] poly(hexyl methacrylate),[4c] polyisoprene,[4f] and polyethylene (PE).[4e,7]

Besides linear macromolecules, dendrimers with a core−shell architecture are attractive as amphilphiles and self-assembling materials due to notable features like well-defined molecular weight and shape persistence.[8] Considering the synthetic approach to an amphiphilic dendrimer, the synthesis of the dendritic core is more difficult than that of the shell due to the branched architecture. This is why only a few chemically distinct dendritic cores of amphiphilic dendrimers have been reported in the literature.[9] Among them, aliphatic amines as poly(amidoamine) (PAMAM) and poly(propyleneimine) (PPI) are most common and have been used in combination with hydrophobic coils in the construction of nanoassembling materials in solution, in the bulk state, and at the air−water interface.[9a−e] To utilize these aliphatic amines as hydrophilic dendritic cores, chemical modifications have been performed to increase their hydrophilicity, leading to well-defined microphase separation. For example, Meijer et al. functionalized hydrophilic carboxylic acid groups onto the surface of PPI or protonated the amine functional groups.[9b,c] Crooks et al. introduced ion pairs between the hydrophobic alkyl chains and the PAMAM dendritic core through acid−base chemistry, which prevents both blocks from mixing.[3c] However, pristine aliphatic amine-based dendritic cores are considered to be hydrophobic rather than hydrophilic. For example, Hammond et al. have used PAMAM as a hydrophobic dendritic block with linear coil-type chains in diblock copolymers which can form ultrathin layered films.[9d,e] Meijer et al. have pointed out the hydrophobic character of amine-terminated PPI in their polystyrene−PPI dendritic polymers which did not show any microphase separation between polystyrene and PPI in the bulk.[9c]

Comparing linear block copolymer and dendritic macromolecular systems strongly suggests the use of PEO/polyether-type dendritic cores for the development of the next-generation dendritic amphiphiles. Surprisingly, to the best of our knowledge, this has not been described in the literature.[10]

In this paper based on the convergent polyether-type dendrimer synthesis devised by Fréchet et al.,[11] we will describe the synthesis of a series of amphiphilic den-

† Present address: Johannes Gutenberg-University, Saarstrasse 21, 55099 Mainz, Germany.

* To whom all correspondence should be addressed. E-mail: ubw1@cornell.edu.

10.1021/ma035745e CCC: $27.50
Published on Web 05/05/2004

Scheme 1. Synthesis of Amphiphilic Dendrimers 1−4

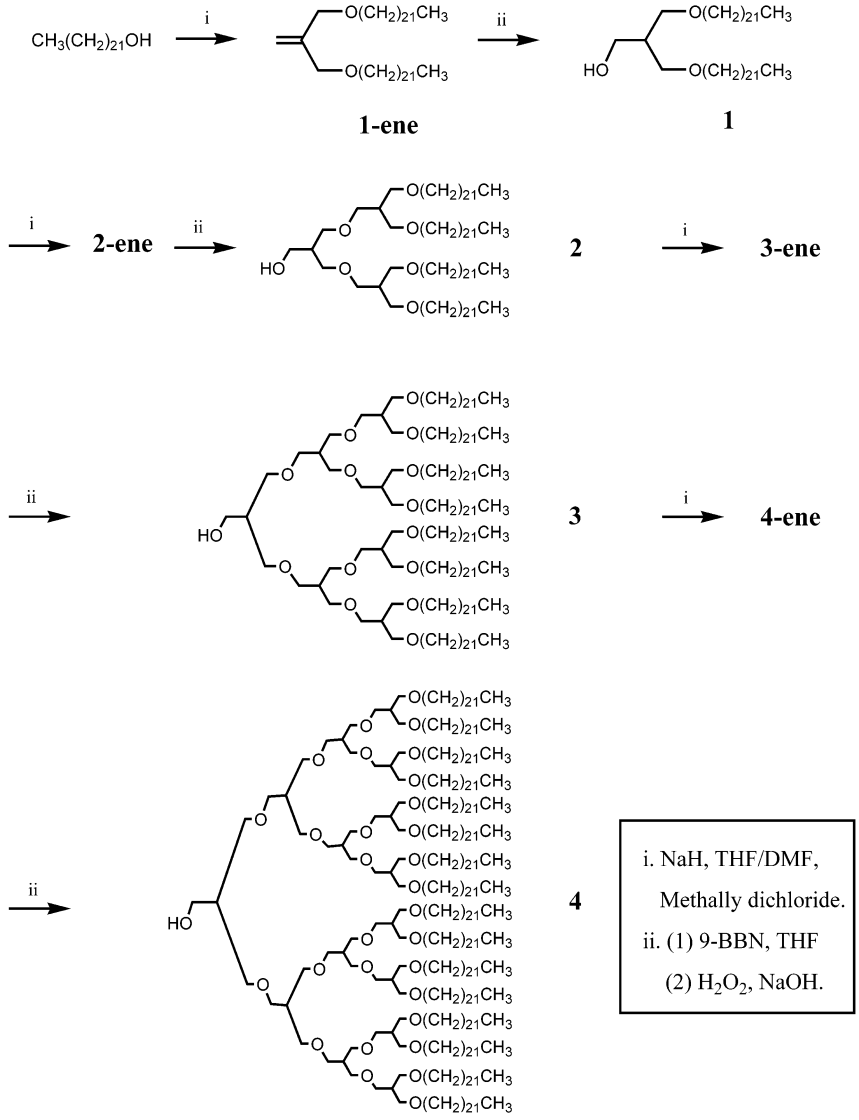

drimer generations **1**−**4** containing a hydrophilic aliphatic polyether-type dendritic core and hydrophobic docosyl peripheries (Scheme 1). After full characterization their self-assembly behavior in the solid state will be elucidated using small-angle X-ray scattering.

Experimental Section

Materials. 1-Docosanol (98%), NaH (95%), 9-BBN (all from Aldrich), and other conventional reagents were used as received. Methallyl dichloride (3-chloro-2-chloromethyl-1-propene) (99%) from Aldrich was distilled and stored over type 4 Å molecular sieve. *N*,*N*-Dimethylformamide (DMF) was distilled under vacuum and stored over type 4 Å molecular sieve. Tetrahydrofuran (THF) was dried by distillation from sodium metal and stored over type 4 Å molecular sieve.

Techniques. ^{1}H NMR spectra were recorded from $CDCl_3$ solutions on a Varian INOVA 300 spectrometer. The purity of the products was checked by thin-layer chromatography (TLC; Merck, silica gel 60). A Perkin-Elmer DSC-7 differential scanning calorimeter equipped with 1020 thermal analysis controller was used to determine the thermal transitions and the heat of fusion. In all cases, the heating and cooling scan rates were 10 °C/min. Gel permeation chromatography (GPC) measurements were carried out in 98% THF and 2% *N*,*N*-dimethylacetamide at ambient temperature using 5 μm Waters Styragel columns (10^3, 10^4, 10^5, 10^6 Å, 30 cm each; Waters Corp., Milford, MA) at a flow rate of 1.0 mL/min. Elemental analysis was performed at Desert Analytics Co. in Tucson, AZ.

Small-angle X-ray scattering measurements were performed in transmission mode with a Rigaku rotating anode X-ray generator (Cu Kα, $\lambda = 1.54$ Å) focused by Franks mirror optics and operated at 40 kV and 50 mA.[12a] A 2-D X-ray detector based on a 512 × 512 pixel Thomson CCD[12b] was used to acquire scattering patterns. The diffraction patterns were concentric powder pattern rings. The raw data were corrected for distortion and nonlinearity of the detector after background subtraction. It was then azimuthally integrated to obtain 1-D plots of intensity vs scattering vector q

$$q = \frac{4\pi}{\lambda}\sin\left(\frac{\theta}{2}\right)$$

where θ is the scattering angle and λ the wavelength of incident radiation.

Wide-angle X-ray diffraction was performed on a Scintag $\theta-\theta$ diffractometer (Cu Kα, $\lambda = 1.54$ Å) operated at 45 kV and 40 mA to determine the crystallinity of docosyl periphery. In the crystallinity determination, the same range of 2θ ($12° < 2\theta < 30°$) was chosen for the analysis of all samples. A common amorphous background was assigned by superimposing the X-ray data of all dendrimers. The crystallinity was then calculated by subtracting the amorphous region from the peak area (see Figure 3).

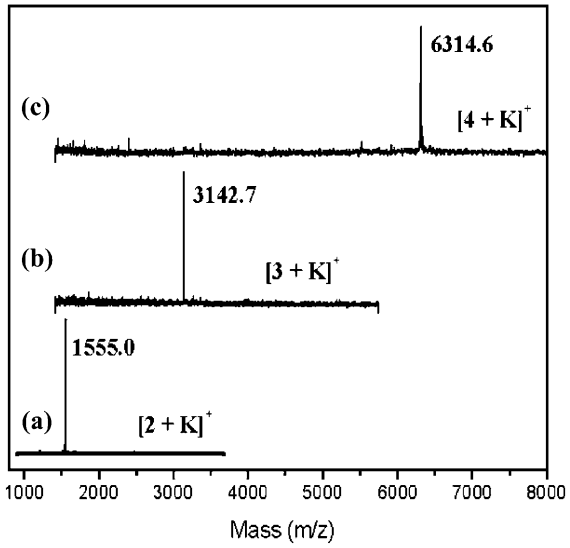

Figure 1. MALDI−TOF MS spectra of (a) **2**, (b) **3**, and (c) **4**.

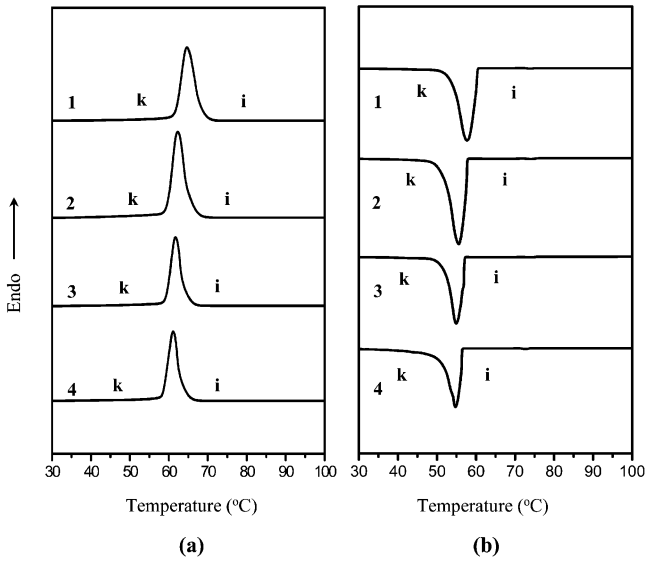

Figure 2. DSC traces (10 °C/min) of amphiphilic dendrimers **1**−**4** recorded during the second heating scan (a) and the first cooling scan (b).

Matrix-assisted laser desorption ionization time-of-flight (MALDI−TOF) mass spectra were recorded using a Bruker Reflex II mass spectrometer (Bremen, Germany) equipped with a N_2 laser ($\lambda = 337$ nm) operating at a pulse rate of 3 Hz. The ions were accelerated with pulsed ion extraction by a voltage of 20 kV and detected using a microchannel plate detector. The analyzer was operated in reflection mode. Sixty shots were accumulated for each mass spectrum. The mass spectrometer was calibrated prior to measurement with a mixture of C_{60} and C_{70} fullerenes. The dendrimer samples were dissolved in THF and mixed with 1,8,9-trihydroxyanthracene (dithranol) and potassium trifluoroacetate in a molar ratio of 1/500/10 (analyte/matrix/salt). Matrix and cationizing salt were purchased from Aldrich (Steinheim, Germany) and used without further purification. The solvent tetrahydrofuran (THF, 99.8%) was obtained from Fluka (Buchs, Switzerland).

Synthesis. The synthesis of the dendrimers is outlined in Scheme 1.

Synthesis of 1-ene. 1-Docosanol (300.0 g, 919 mmol), NaH (36.7 g, 1529 mmol), and methallyl dichloride (63.8 g, 510 mmol) were dissolved in 1000 mL of a THF/DMF solvent mixture. The mixture was heated at reflux for 63 h under N_2 atmosphere and then quenched with water. After cooling to room temperature, the mixture was poured into ethyl acetate.

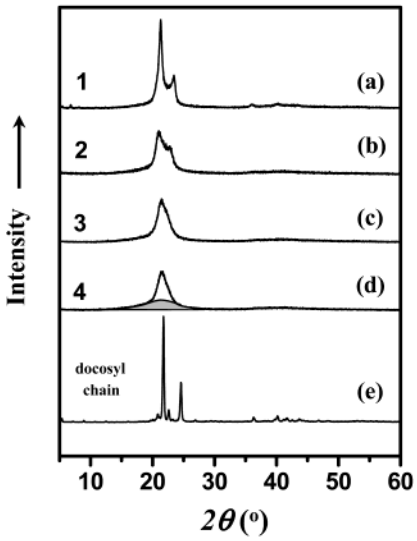

Figure 3. Wide-angle X-ray scattering patterns of dendrimers **1** (a), **2** (b), **3** (c), and **4** (d) in the solid state. WAXS patterns from dendrimers were normalized to the same area of the amorphous halo; see (d). For reference, the pattern of pure docosanol is also depicted; see (e).

The resulting precipitate was collected using a glass filter and passed through a column of silica gel with chloroform as an eluent to remove the dark-brown color. The obtained compound was purified by several recrystallizations from *n*-hexane to yield 194 g (60%) of a white crystal. ^{1}H NMR ($CDCl_3$, δ, ppm): 5.17 (s, 2H), 3.97 (s, 4H), 3.41 (t, 4H, $J = 6.8$ Hz), 1.02−1.70 (m, 80H), 0.89 (t, 6H, $J = 6.8$ Hz); $\bar{M}_w/\bar{M}_n = 1.03$ (GPC).

Synthesis of 1. 1-ene (180 g, 255 mmol) was dissolved in 1000 mL of THF under a N_2 atmosphere, and 800 mL of 0.5 M of 9-BBN solution in THF was added dropwise at room temperature. The reaction mixture was stirred for 45 min, was then cooled to 0 °C in an ice bath, then carefully quenched with 210 mL of 3 M NaOH aqueous solution, and then stirred for 30 min at room temperature. The reaction mixture was cooled again to 0 °C, and 210 mL of 30% H_2O_2 aqueous solution was carefully added. The mixture was stirred at room temperature 3 h, and THF was then removed in a rotary evaporator. The mixture was saturated with K_2CO_3 and extracted with chloroform. After removing chloroform in a rotary evaporator, the resulting solid was purified by several recrystallizations from ethyl acetate to yield 175 g (95%) of a white solid. ^{1}H NMR ($CDCl_3$, δ, ppm): 3.77 (m, 2H), 3.53 (m, 4H), 3.42 (t, 4H, $J = 6.8$ Hz), 2.13 (m, 1H), 1.02−1.70 (m, 80H), 0.89 (t, 6H, $J = 6.8$ Hz). Anal. Calcd for $C_{48}H_{98}O_3$: C, 79.71; H, 13.66. Found: C, 79.70; H, 13.36; $\bar{M}_w/\bar{M}_n = 1.03$ (GPC).

Synthesis of 2-ene. 1 (175.0 g, 242 mmol), NaH (10.3 g, 431 mmol), and methallyl dichloride (16.8 g, 135 mmol) were dissolved in 600 mL of a THF/DMF solvent mixture. The mixture was heated at reflux for 26 h under a N_2 atmosphere and then quenched with water. After cooling to room temperature, the mixture was poured into ethyl acetate. The resulting precipitate was collected using a glass filter and passed through a column of silica gel with chloroform as an eluent to remove the dark-brown color. The obtained compound was purified by several recrystallizations from a *n*-hexane:ethyl acetate = 1:2 solvent mixture to yield 120 g (66%) of a white crystal. ^{1}H NMR ($CDCl_3$, δ, ppm): 5.15 (s, 2H), 3.95 (s, 4H), 3.35−3.52 (m, 20H), 2.16 (m, 2H), 1.02−1.70 (m, 160H), 0.89 (t, 12H, $J = 6.8$ Hz); $\bar{M}_w/\bar{M}_n = 1.04$ (GPC).

Synthesis of 2. 2-ene (120 g, 80 mmol) was dissolved in 500 mL of THF under a N_2 atmosphere, and 240 mL of 0.5 M of 9-BBN solution in THF was added dropwise at room temperature. The reaction mixture was stirred for 45 min, cooled to 0 °C in an ice bath, then carefully quenched with 67 mL of 3 M NaOH aqueous solution, and stirred for 30 min at room temperature. The reaction mixture was cooled again to 0 °C, and 67 mL of 30% H_2O_2 aqueous solution was carefully

Table 1. Characterization of Dendrimers

amphiphilic dendrimer	mol wt (g/mol)		weight fraction of docosyl periphery	crystallinity of PE (%)		correlation length	melting transitions (°C) and corresponding enthalpy changes (J/g)	
	a	*b*	*f*(docosyl)	*c*	*d*	*t* (nm)[e]	heating[f]	cooling
1	723.3		0.86	56.5	61.1	24.0	k 65.6 (141.2) i k 64.6 (140.8) i	k 57.7 (140.1) i
2	1516.7	1515.9	0.82	51.1	53.2	12.2	k 62.6 (121.8) i k 62.3 (118.2) i	k 55.6 (118.4) i
3	3103.4	3103.6	0.80	49.8	50.1	8.8	k 61.7 (116.1) i k 61.7 (113.1) i	k 54.9 (113.2) i
4	6276.9	6275.5	0.79	44.9	45.8	8.1	k 61.1 (103.5) i k 61.1 (103.4) i	k 54.7 (100.7) i

[a] Theoretical molecular weight. [b] Determined by MALDI−TOF MS. [c] Calculated from heats of fusion on the first heating. Degree of crystallinity = experimental heat of fusion of a single docosyl group/heat of fusion of a perfect crystalline docosyl group. Experimental heat of fusion of a single docosyl group (kJ/mol) = heat of fusion (J/g) from first heating × mass of a single docosyl group (309.6 g/mol)/*f*(docosyl). The heat of fusion of a single perfect crystalline docosyl group is 90.4 kJ/mol and was calculated from the heat of fusion of a methylene unit in the perfect crystalline polyethylene of 4.11 kJ/mol. [d] Calculated from wide-angle X-ray diffraction. [e] Correlation length (t) = $0.9\lambda/(B \cos \theta_B)$, where λ is the wavelength of the X-ray beam (Kα = 0.154 nm), B is an angular width at half the maximum intensity, and $2\theta_B$ is a scattering angle. [f] For each generation, the isotropic temperature was obtained from the first (first value) and second (second value) heating scans (k = crystal, i = isotropic liquid).

added. The mixture was stirred for 3 h at room temperature, and THF was then removed in a rotary evaporator. The mixture was saturated with K_2CO_3 and extracted with chloroform. After removing chloroform in a rotary evaporator, the resulting solid was purified by several recrystallizations from ethyl acetate to yield 117 g (96%) of a white solid. ^{1}H NMR ($CDCl_3$, δ, ppm): 3.74 (m, 2H), 3.30−3.60 (m, 24H), 2.13 (m, 3H), 1.02−1.70 (m, 160H), 0.89 (t, 12H, J = 6.8 Hz). MS (MALDI−TOF): m/z calcd for ($C_{100}H_{202}O_7$) 1516.67; found 1515.89. Anal. Calcd for $C_{100}H_{202}O_7$: C, 79.19; H, 13.42. Found: C, 78.85; H, 13.26; $\bar{M}_w/\bar{M}_n$ = 1.04 (GPC).

Synthesis of 3-ene. 2 (83 g, 55 mmol), NaH (1.8 g, 76 mmol), and methallyl dichloride (3.8 g, 30.4 mmol) were dissolved in 400 mL of a THF/DMF solvent mixture. The mixture was heated at reflux for 26 h under a N_2 atmosphere and then quenched with water. After cooling to room temperature, the mixture was poured into ethyl acetate. The resulting precipitate was collected using a glass filter and passed through a column of silica gel with chloroform as an eluent to remove the dark-brown color. The obtained compound was purified by several recrystallizations from a *n*-hexane:ethyl acetate = 1:2 solvent mixture to yield 62 g (66%) of a white solid. ^{1}H NMR ($CDCl_3$, δ, ppm): 5.17 (s, 2H), 3.93 (s, 4H), 3.22−3.60 (m, 52H), 2.16 (m, 6H), 0.80−1.62 (m, 344); $\bar{M}_w/\bar{M}_n$ = 1.03 (GPC).

Synthesis of 3. 3-ene (61.5 g, 20 mmol) was dissolved in 500 mL of THF under a N_2 atmosphere, and 60 mL of 0.5 M of 9-BBN solution in THF was added dropwise at room temperature. The reaction mixture was stirred for 45 min, cooled to 0 °C in an ice bath, then carefully quenched with 17 mL of 3 M NaOH aqueous solution, and then stirred for 30 min at room temperature. The reaction mixture was cooled again to 0 °C, and 17 mL of 30% H_2O_2 aqueous solution was carefully added. The mixture was stirred for 3 h at room temperature, and THF was then removed in a rotary evaporator. The mixture was saturated with K_2CO_3 and extracted with chloroform. After removing chloroform in a rotary evaporator, the resulting solid was purified by several recrystallizations from a *n*-hexane:ethyl acetate = 1:2 solvent mixture to yield 59 g (95%) of a white solid. ^{1}H NMR ($CDCl_3$, δ, ppm): 3.72 (d, 2H, J = 5.0 Hz), 3.20−3.60 (m, 56H), 2.13 (m, 7H), 0.80−1.65 (m, 344). MS (MALDI−TOF): m/z calcd for ($C_{204}H_{410}O_{15}$) 3103.43; found 3102.77. Anal. Calcd for $C_{204}H_{410}O_{15}$: C, 78.95; H, 13.32. Found: C, 78.86; H, 13.08; $\bar{M}_w/\bar{M}_n$ = 1.02 (GPC).

Synthesis of 4-ene. 3 (50 g, 16.2 mmol), NaH (0.58 g, 24.3 mmol), and methallyl dichloride (1.0 g, 8.1 mmol) were dissolved in 200 mL of a THF/DMF solvent mixture. The mixture was heated at reflux for 30 h under a N_2 atmosphere and then quenched with water. After cooling to room temperature, the mixture was poured into ethyl acetate. The resulting precipitate was collected using a glass filter and passed through a column of silica gel with chloroform as an eluent to remove the dark-brown color. The obtained compound was purified by several recrystallizations from a *n*-hexane:ethyl acetate = 1:1 solvent mixture to yield 28 g (55%) of a white solid. ^{1}H NMR ($CDCl_3$, δ, ppm): 5.17 (s, 2H), 3.91 (s, 4H), 3.10−3.70 (m, 116H), 2.13 (m, 14H), 0.80−1.67 (m, 688); $\bar{M}_w/\bar{M}_n$ = 1.03 (GPC).

Synthesis of 4. 4-ene (21.0 g, 3.4 mmol) was dissolved in 300 mL of THF under a N_2 atmosphere, and 50 mL of a 0.5 M of 9-BBN solution in THF was added dropwise at room temperature. The reaction mixture was stirred for 45 min, then cooled to 0 °C in an ice bath, then carefully quenched with 11 mL of 3 M NaOH aqueous solution, and then stirred for 30 min at room temperature. The reaction mixture was cooled again to 0 °C, and 11 mL of 30% H_2O_2 aqueous solution was carefully added. The mixture was stirred for 3 h at room temperature, and then THF was removed in a rotary evaporator. The mixture was saturated with K_2CO_3 and extracted with chloroform. After removing chloroform in a rotary evaporator, the resulting solid was purified by several recrystallizations from a *n*-hexane:ethyl acetate = 1:2 solvent mixture to yield 19.5 g (93%) of a white solid. ^{1}H NMR ($CDCl_3$, δ, ppm): 3.72 (d, 2H, J = 5.0 Hz), 2.98−3.62 (m, 120H), 2.13 (m, 15H), 0.80−1.65 (m, 688). MS (MALDI−TOF): m/z calcd for ($C_{412}H_{826}O_{31}$) 6276.95, found 6275.46. Anal. Calcd for $C_{412}H_{826}O_{31}$: C, 78.83; H, 13.26. Found: C, 78.82; H, 13.54; $\bar{M}_w/\bar{M}_n$ = 1.02 (GPC).

Results and Discussion

Synthesis and Characterization. The present design of amphiphilic dendrimers was focused on the construction of a PEO-like aliphatic dendritic core. This chemistry should provide a stronger hydrophilic character than observed for the more common poly(benzyl ether) dendritic cores. As shown in Scheme 1, the repeat unit of the aliphatic dendritic core is $CH_2CH(CH_2O)_2$. With respect to molecular composition, this is almost identical to twice a linear PEO repeat unit: 2 × (CH_2CH_2O). As a hydrophobic periphery, a docosyl group with 22 methylene units was employed in order to provide maximum incompatibility with the hydrophilic dendritic core. The basic synthetic methodology to generate such amphiphilic dendrimers employs a facile convergent route developed by the Fréchet group in order to control the dendritic architecture precisely.[11] The first growth step is performed by a Williamson etherification reaction of an alcoholic precursor in each generation with methallyl dichloride, while the activation step of the resulting olefin is carried out through a hydroboration−oxidation reaction. All the dendrimers **1**−**4** have been obtained in good yields and high purity as described in the Experimental Section. The synthetic procedure is outlined in Scheme 1. The etherification

reaction of the primary alcoholic precursor in each generation with methallyl dichloride was performed in a THF/DMF solvent mixture and NaH as base. For comparison, THF or DMF was also used individually as solvents for the etherification reaction under the same experimental conditions, but only very poor yields (<10%) were observed. In the THF/DMF solvent mixture, polar DMF can be considered to play a better role in dissociating the oxyanion and sodium cation than pure THF, which facilitates the nucleophilic attack of the oxyanion toward methallyl chloride, resulting in high yields. On the other hand, the PE units show poor solubility in pure DMF, and this reaction therefore results in a poor yield. In all the etherification reactions, the DMF volume fraction was 30%. Because of the crystalline nature of docosyl peripheries, the purifications of the olefins **1-ene**, **2-ene**, **3-ene**, and **4-ene** were performed simply using repetitive recrystallizations from hexanes−ethyl acetate mixtures with various compositions depending on the generation. This afforded yields between 55% and 66% for all generations. The purity of each olefin compound was checked using GPC and NMR techniques. The polydispersity of the molecular weights of all the olefin compounds as determined by GPC is less than 1.04. In addition, NMR data are in full agreement with the expected structures in which the characteristic two singlet peaks corresponding to the olefinic protons and the allylic protons appear at 5.2 and 3.9 ppm, respectively.[11b] On the other hand, the activation step was achieved by a hydroboration−oxidation reaction with 9-BBN as the borane reagent which expels unwanted tertiary alcohol due to its high steric hindrance. Purification of the resulting dendrimers **1**−**4** with primary alcoholic groups was carried out using repetitive recrystallizations from a hexanes−ethyl acetate mixture and gave high yields (>90%) in all cases. The amphiphilic dendrimers **1**−**4** were characterized by NMR, GPC, and elemental analysis. All dendrimers show narrow polydispersities of less than 1.03 in GPC and give signals for the α-protons to the hydroxy group at 3.7 ppm and methine protons at 2.1 ppm in the NMR spectra.[11b] Elemental analysis data of **1**−**4** are also in good agreement with the theoretical values.

Molecular weights (MWs) of **2**, **3**, and **4** were determined by MALDI−TOF MS (Table 1 and Figure 1). In all cases, only a single peak corresponding to [dendrimer + K]$^+$ was observed, and the calculated MWs based on the peak positions are in good agreement with the theoretical MWs (see Table 1), confirming the successful synthesis of the amphiphilic dendrimers in high purity.

Thermal Properties and Degree of Crystallinity. Thermal properties like melting transitions and heats of fusion of the amphiphilic dendrimers **1**−**4** were determined by differential scanning calorimetry (DSC). All the heating and cooling scans were performed at a rate of 10 °C/min. As shown in Figure 2, only a single peak (i.e., no glass transition) is observed in both heating and cooling scans of **1**−**4**, which corresponds to a transition from solid to isotropic liquid. It can be attributed to the melting transition of the docosyl peripheries because the hydrophilic dendritic core is not expected to crystallize due to its branched architecture. The position of the melting transitions as well as the heats of fusion of the docosyl peripheries decreases slightly from generation to generation. The melting behavior also demonstrates that the hydrophobic region is well-segregated from the hydrophilic dendritic core

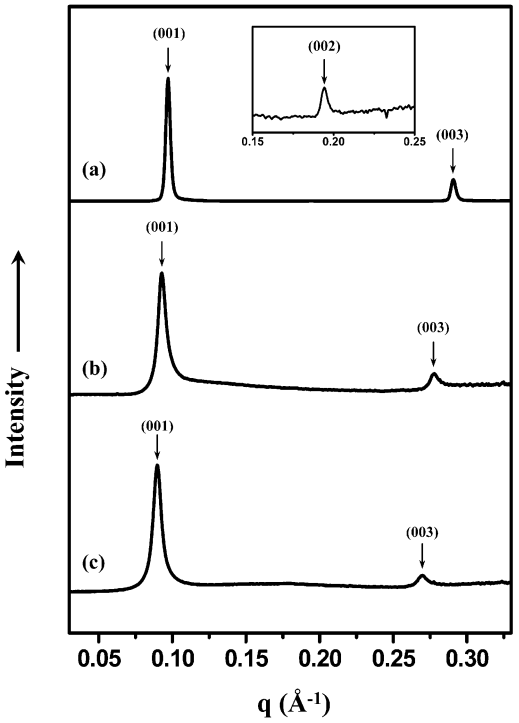

Figure 4. Small-angle X-ray scattering patterns of **1** (a), **2** (b), and **3** (c) in the solid state. The tic marks are for a lamellar lattice. The inset of (a) shows the magnified (×70) (002) reflection.

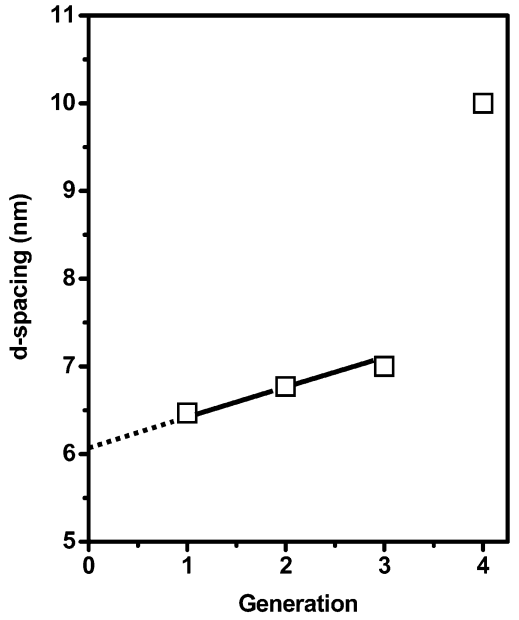

Figure 5. Dependence of *d* spacing of primary peak on generation.

region. The melting temperatures and heats of fusion on both first and second heating scans are almost identical, indicating that the crystallization of the docosyl periphery occurs reversibly at the rate of 10 °C on heating and cooling. The degree of crystallinity of the docosyl peripheries in **1**−**4** can be determined by comparing the heats of fusion on the first heating to that of a perfect crystalline PE (Table 1).[13] It decreases gradually from 56% to 45% with increasing generation. Alternatively, wide-angle X-ray scattering (WAXS) was employed to estimate the degree of crystallinity. To this end, Figure 3 shows room temperature WAXS spectra for all dendrimers **1**−**4** in comparison to the correspond-

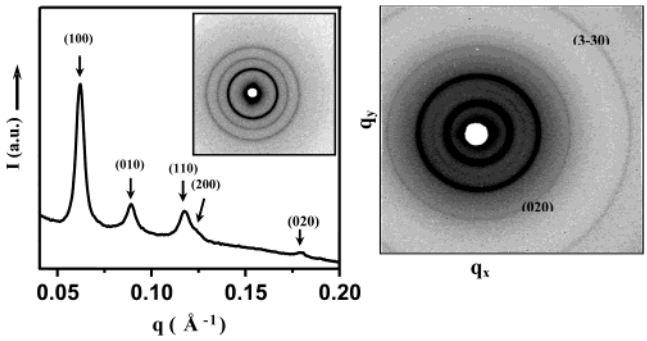

Figure 6. Small-angle X-ray scattering patterns of **4** in the solid state. (a) Pattern obtained through azimuthal integration of the full 2D diffractogram (see inset) and exhibiting five of the six reflections observed for this compound. This pattern was collected with a sample-to-detector distance of 59.4 cm. Prior to data collection, the sample was annealed for about 24 h at 55 °C. (b) 2D diffractogram obtained with a sample-to-detector distance of 40.7 cm. Prior to data collection, this sample was annealed for only an hour, resulting in a variation of peak intensities compared to (a). For these conditions a sixth peak indexed (3−30) can clearly be identified at high q values.

ing spectrum of the parent docosanol. Dendrimer spectra were normalized to the same area of the amorphous halo (see shaded area in spectrum d of Figure 3) to allow for quantitative comparison of the degree of crystallinity. As is obvious, the crystallinity decreases gradually with increasing generation. Quantitative analysis shows good agreement with the DSC results (see Table 1). On the basis of the line width of the peaks at around 21.5° (2θ) in the WAXS spectra, the correlation length, t, could be determined to estimate the lateral regularity of docosyl peripheries as a function of dendrimer generation (Table 1).[14] The correlation length decreases significantly from **1** to **2** and then only gradually reduces further with generation. It is interesting to note that for generations **1**−**3** the correlation length is larger than the lamellar spacing (see next section), indicating that crystalline lamellar hydrocarbon sheets are separated by amorphous PEO-type dendritic cores. All these trends can be explained considering interfacial curvature arising from the molecular shape as a function of the generation. It is well-known that the shape of a dendrimer approaches more and more a globular shape with each generation.[5] Thus, the interface between the hydrophobic docosyl periphery and hydrophilic dendritic core changes from a more flat surface to a curved surface, causing a large interfacial area and resulting in the reduction of the melting transition and heat of fusion.

Amphiphilic Dendrimer Self-Assembly. As concluded form the thermal properties, the present dendritic amphiphile architecture with PEO-type dendritic cores and PE-like docosyl peripheries leads to segregation between hydrophilic and hydrophobic moieties. To investigate this self-assembly behavior in more detail, small-angle X-ray scattering (SAXS) experiments have been performed in the solid state. Compounds **1**−**3** exhibit very similar SAXS patterns (Figure 4), showing two strong reflections with position ratios of 1:3. The weak intensity or lack of a second-order peak might be due to the degree of crystallinity of about 50%, leading to a minimum in the structure factor (F) of **1**−**3** at that position. This could be confirmed by separate Fourier transformations of electron density profiles consisting of three blocks corresponding to amorphous docosyl periphery, crystalline docosyl periphery, and dendritic core. In these model calculations, simply assuming electron densities proportional to mass densities, indeed F^2 of the second-order peak showed a relatively weak intensity for dendrimer compositions **1**−**3** and their respective degrees of crystallinities as observed by DSC/XRD.

From the observed primary peak, d spacings for **1**, **2**, and **3** can be estimated to be 6.5, 6.8, and 7.0 nm, respectively. In Figure 5, the d spacing is plotted as a function of generation, suggesting a linear dependence for **1**−**3**. Extrapolation to zero generation results in a d spacing of about 6 nm. This value can be considered as the hypothetical lamellar dimension constructed from docosyl blocks since only the dendritic core length increases as a function of the generation. Since the fully stretched length of docosyl as calculated from the Corey−Pauling−Koltun (CPK) model is approximately 3 nm, it can be concluded that **1**−**3** are self-organized into a bilayered lamellar structure rather than an interdigitated lamellar structure in the solid state. This result can be easily rationalized since a bilayer configuration is more suitable to minimize interfacial area. On the other hand, the increase in periodicity derived from the d spacing is 0.3 nm from **1** to **2** and 0.2 nm from **2** to **3**. These values are significantly smaller than 0.47 nm, corresponding to the increase of length of the dendritic core edge when moving to the next generation as calculated from the CPK model. Therefore, the hydrophilic dendritic cores probably pack in a somewhat interdigitated fashion and distort conformationally. Considering the space-filling requirement and taper-shaped dendrimer, the interdigitated fashion is expected to be the best way to close-pack the dendritic cores while

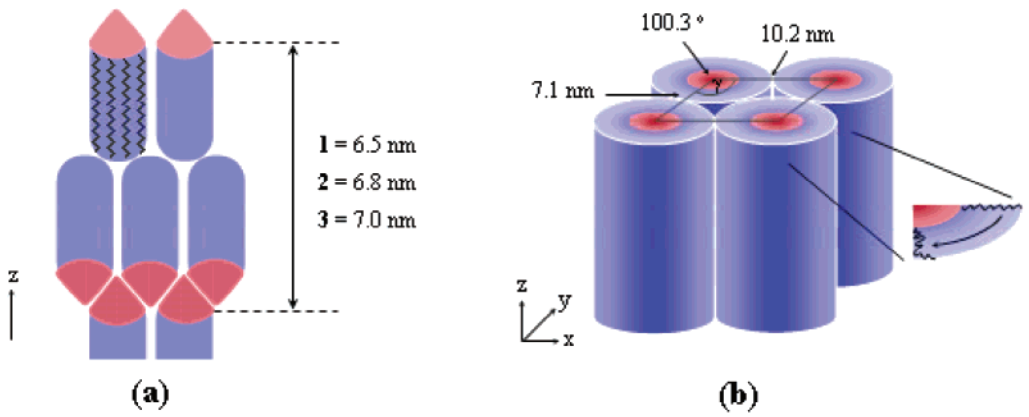

Figure 7. Schematic representation of (a) the bilayered lamellar morphology of **1**, **2**, and **3** and (b) the 2-dimensional oblique columnar morphology of **4**.

maintaining the bilayered lamellar structure (Figure 7a).

The amphiphilic dendrimer **4** does not follow the linear trends in structure of the smaller homologues. The SAXS pattern of this compound shows six peaks (the sixth peak at high q values was only observed by going to a shorter sample-to-detector distance; see Figure 6b and caption). The d spacing of 10.0 nm estimated from the primary peak in the SAXS pattern of this compound (Figure 6) deviates far from the expected value obtained from a linear extrapolation of the data of generations **1**−**3** (see Figure 5). Furthermore, this SAXS pattern does not fit to a conventional lamellar lattice. It was analyzed in terms of a general oblique planar lattice. The equation for peak positions for such a lattice in reciprocal space is given by[15]

$$\frac{q^2}{(2\pi)^2} = \frac{h^2}{(a \sin \gamma)^2} - \frac{2hk \cos \gamma}{ab \sin^2 \gamma} + \frac{k^2}{(b \sin \gamma)^2} \quad (1)$$

where h and k are Miller indices of the scattering planes, a and b are unit cell basis vectors, and γ is the angle between a and b ($0° < \gamma < 180°$).

Using this relation, the six peaks could be consistently indexed as (100), (010), (110), (200), (020), and (3−30), which agrees with a 2-dimensional oblique columnar lattice with lattice parameters $a = 10.2$ nm, $b = 7.1$ nm, and $\gamma = 100.3°$. Based on the CPK model, the length of the fully stretched molecule from focal point to docosyl chain end is approximately 5.0 nm. This suggests that dendritic cores as well as docosyl peripheries pack in a noninterdigitated fashion. Considering the taper-shaped molecular architecture of **4** with highly curved interface, **4** can be considered to form a cylinder more preferentially than the other dendrimers, also consistent with earlier findings.[8d−h] Thus, from the SAXS results and assuming a noninterdigitated molecular packing, we propose a structure in which the amphiphilic dendrimer **4** self-assembles into columns packed into an oblique lattice, as illustrated in Figure 7b. The cross section of the column can be considered elliptical instead of circular to satisfy the nonsymmetrical oblique packing of columns. The driving force for this distortion of the cross section is attributed to the crystallization of docosyl peripheries, similar to what was found in another system.[16] At this point, we speculate that docosyl chains are more crystalline along the longer axis of the elliptical cross section than along the shorter axis, as illustrated in the sketch in Figure 7b.

Conclusions

A novel series of amphiphilic dendrimer generations **1**−**4** with hydrophilic aliphatic polyether-type dendrimer cores and hydrophobic docosyl peripheries have been synthesized in high purity and yield by iterative Williamson etherification and hydroboration/oxidation reactions. Melting transitions and corresponding heats of fusion of docosyl peripheries decrease slightly as a function of generation. Structural parameters of **1**−**3** in the solid state are consistent with bilayered lamellar structures with interdigitated dendritic core packing. In marked contrast, X-ray data of **4** suggest a 2-dimensional oblique columnar arrangement. The thermal and morphological properties can be rationalized in terms of microphase separation between hydrophilic dendritic core and hydrophobic docosyl peripheries and the change of molecular architecture and interfacial curvature from generation to generation. Because of its chemical nature, i.e., a PEO-like core, and its high hydrophilicity and chemical stability, this novel system may overcome a number of short comings of previous dendritic amphiphiles and therefore holds scientific as well as technological promise in areas ranging from microelectronics all the way to nanobiotechnology. Work along these lines is now in progress in our laboratories.

Acknowledgment. This work was supported by the Post-doctoral Fellowship Program of Korea Science & Engineering Foundation (KOSEF) and the National Science Foundation (DMR-0312913). Financial support of Philip Morris, USA, is gratefully acknowledged. The SAXS X-ray facility is supported by Department of Energy BER Grant DE-FG02-97ER62443. The work was further supported by the Cornell Center for Materials Research (CCMR), a Materials Research Science and Engineering Center of the National Science Foundation (DMR-0079992).

References and Notes

(1) (a) Joester, D.; Losson, M.; Pugin, R.; Heinzelmann, H.; Walter, E.; Merkle, H. P.; Diederich, F. *Angew. Chem., Int. Ed.* **2003**, *42*, 1486. (b) Stiriba, S. E.; Frey, H.; Haag, R. *Angew. Chem., Int. Ed.* **2002**, *41*, 1329. (c) Krämer, M.; Stumbé, J.-F.; Türk, H.; Krause, S.; Ansgar, K.; Delineau, L.; Prokhorova, S.; Kautz, H.; Haag, R. *Angew. Chem., Int. Ed.* **2002**, *41*, 4252. (d) Gillies, E. R.; Fréchet, J. M. J. *Chem. Commun.* **2003**, 1640.

(2) (a) Sone, E. D.; Zubarev, E. R.; Stupp, S. I. *Angew. Chem., Int. Ed.* **2002**, *41*, 1706. (b) Zhao, D.; Feng, J.; Huo, Q.; Melosh, N.; Fredrickson, G. H.; Chmelka, B. F.; Stucky, G. D. *Science* **1998**, *279*, 548. (c) Cha, J. N.; Stucky, G. D.; Morse, D. E.; Deming, T. J. *Nature (London)* **2000**, *403*, 289. (d) Simon, P. F. W.; Ulrich, R.; Spiess, H. W.; Wiesner, U. *Chem. Mater.* **2001**, *12*, 3464. (e) Bagshaw, S. A.; Prouzet, E.; Pinnavaia, T. J. *Science* **1995**, *269*, 1242. (f) Hartgerink, J. D.; Beniash, E.; Stupp, S. I. *Science* **2001**, *294*, 1684.

(3) (a) Piotti, M. E.; Rivera, F.; Bond, R.; Hawker, C. J.; Fréchet, J. M. J. *J. Am. Chem. Soc.* **1999**, *121*, 9471. (b) Boerakker, M. J.; Hannink, J. M.; Bomans, P. H. H.; Frederik, P. M.; Nolte, R. J. M.; Meijer, E. M.; Sommerdijk, N. A. J. M. *Angew. Chem., Int. Ed.* **2002**, *41*, 4239. (c) Chechik, V.; Zhao, M.; Crooks, R. M. *J. Am. Chem. Soc.* **1999**, *121*, 4910.

(4) (a) Göltner, C. G.; Henke, S.; Weissenberger, M. C.; Antonietti, M. *Angew. Chem., Int. Ed.* **1998**, *37*, 613. (b) Yu, K.; Hurd, A. J.; Eisenberg, A.; Brinker, C. J. *Langmuir* **2001**, *17*, 7961. (c) Mahajan, S.; Renker, S.; Simon, P. F. W.; Gutmann, J. S.; Jain, A.; Gruner, S. M.; Fetters, L. J.; Coates, G. W.; Wiesner, U. *Macromol. Chem. Phys.* **2003**, *204*, 1047. (d) Hillmyer, M. A.; Bates, F. S.; Almdal, K.; Mortensen, K.; Ryan, A. J.; Fairclough, J. P. A. *Science* **1996**, *271*, 976. (e) Hillmyer, M. A.; Bates, F. S. *Macromolecules* **1996**, *29*, 6994. (f) Templin, M.; Franck, A.; Chesne, A. D.; Leist, H.; Zhang, Y.; Ulrich, R.; Schädler, V.; Wiesner, U. *Science* **1997**, *278*, 1795.

(5) (a) Wright, P. V.; Zheng, Y. In *Functional Organic and Polymeric Materials*; Richardson, T. H., Ed.; Wiley-VCH: New York, 1998; pp 233−271. (b) Dias, F. B.; Batty, S. V.; Gupta, A.; Ungar, G.; Voss, J. P.; Wright, P. V. *Electrochim. Acta* **1998**, *43*, 1217. (c) Ohtake, T.; Ogasawara, M.; Ito-Akita, K.; Nishina, N.; Ujiie, S.; Ohno, H.; Kato, T. *Chem. Mater.* **2000**, *12*, 782. (d) Kishimoto, K.; Yoshio, M.; Mukai, T.; Yoshizawa, M.; Ohno, H.; Kato, T. *J. Am. Chem. Soc.* **2003**, *125*, 3196.

(6) Gref, R.; Minamitake, Y.; Paracchia, M. T.; Trubeskoy, V.; Torchilin, V.; Langer, R. *Science* **1994**, *263*, 1600.

(7) Lu, Y.; Hu, Y.; Wang, Z. M.; Manias, E.; Chung, T. C. *J. Polym. Sci., Part A: Polym. Chem.* **2002**, *40*, 3416.

(8) (a) Zeng, F. W.; Zimmenerman, S. C. *Chem. Rev.* **1997**, *97*, 1681. (b) Bosman, A. W.; Janssen, H. M.; Meijer, E. W. *Chem. Rev.* **1999**, *99*, 1665. (c) Grayson, S. M.; Fréchet, J. M. J. *Chem. Rev.* **2001**, *101*, 3819. (d) Hudson, S. D.; Jung, H.-T.; Percec, V.; Cho, W.-D.; Johansson, G.; Ungar, G.; Balagurusamy, V. S. K. *Science* **1997**, *278*, 449. (e) Percec, V.; Cho, W.-D.; Mosier, P. E.; Ungar, G.; Yeardley, D. J. P. *J. Am. Chem. Soc.* **1998**, *120*, 11061. (f) Percec, V.; Cho, W. D.;

Ungar, G.; Yeardley, D. J. P. *Angew. Chem., Int. Ed.* **2000**, *39*, 1597. (g) Percec, V.; Glodde, M.; Bera, T. K.; Miura, Y.; Shiyanovskaya, I.; Singer, K. D.; Balagurusamy, V. S. K.; Heiney, P. A.; Schnell, I.; Rapp, A.; Spiess, H.-W.; Hudson, S. D.; Duan, H. *Nature (London)* **2002**, *419*, 384. (h) Ungar, G.; Liu, Y.; Zeng, X.; Percec, V.; Cho, W. D. *Science* **2003**, *299*, 1208.

(9) (a) Schenning, A. P. H. J.; Elissen-Román, C.; Weener, J.-W.; Baars, M. W. P. L.; van der Gaast, S. J.; Meijer, E. W. *J. Am. Chem. Soc.* **1998**, *120*, 8199. (b) van Hest, J. C. M.; Baars, M. W. P. L.; Elissen-Román, C.; van Genderen, M. H. P.; Meijer, E. W. *Macromolecules* **1995**, *28*, 6689. (c) Román, C.; Fischer, H. R.; Meijer, E. W. *Macromolecules* **1999**, *32*, 5525. (d) Iyer, J.; Fleming, K.; Hammond, P. T. *Macromolecules* **1998**, *31*, 8757. (e) Iyer, J.; Hammond, P. T. *Langmuir* **1999**, *15*, 1299. (f) Lorenz, K.; Frey, H.; Stühn, B.; Mülhaupt, R. *Macromolecules* **1997**, *30*, 6860. (g) Cameron, J. H.; Facher, A.; Lattermann, G.; Diele, S. *Adv. Mater.* **1997**, *9*, 398. (h) Kim, C.; Kim, K. T.; Chang, Y.; Song, H. H.; Jeon, H.-J. *J. Am. Chem. Soc.* **2001**, *123*, 5586. (i) Gitsov, I.; Wooley, K. L.; Hawker, C. J.; Ivanova, P. T.; Fréchet, J. M. J. *Macromolecules* **1993**, *26*, 5621.

(10) Linear and cyclic oligo(ethylene oxide) groups have been placed at the root of the dendron: (a) Johannson, G.; Percec, V.; Ungar, G.; Abramic, D. *J. Chem. Soc., Perkin Trans. 1* **1994**, 447. (b) Percec, V.; Heck, J.; Tomazos, D.; Falkenberg, F.; Blackwell, H.; Ungar, G. *J. Chem. Soc., Perkin Trans. 1* **1993**, 2799. (c) Percec, V.; Heck, J.; Tomazos, D.; Ungar, G. *J. Chem. Soc., Perkin Trans. 2* **1993**, 2381.

(11) (a) Jayaraman, M.; Fréchet, J. M. J. *J. Am. Chem. Soc.* **1998**, *120*, 12996. (b) Grayson, S. M.; Fréchet, J. M. J. *J. Am. Chem. Soc.* **2000**, *122*, 10335.

(12) (a) Finnefrock, A. C.; Ulrich, R.; Toombes, G. E. S.; Gruner, S. M.; Wiesner, U. *J. Am. Chem. Soc.* **2003**, *125*, 13084. (b) Tate, M. W.; Gruner, S. M.; Eikenberry, E. F. *Rev. Sci. Instrum.* **1997**, *68*, 47.

(13) Loo, Y. L.; Register, R. A.; Adamson, D. H. *J. Polym. Sci., Part B: Polym. Phys.* **2000**, *38*, 2564.

(14) Cullity, B. D. *Elements of X-ray Diffraction*, 2nd ed.; Addison-Wesley: Reading, MA, 1978.

(15) Li, X.; Hirsh, D. J.; Carbral-Lilly, D.; Zirkel, A.; Gruner, S. M.; Janoff, A. S.; Perkins, W. R. *Biochim. Biophys. Acta* **1998**, *1415*, 23.

(16) Luedtke, W. D.; Landman, U. *J. Phys. Chem.* **1996**, *100*, 13323.

MA035745E